Energy Advances

ROYAL SOCIETY OF CHEMISTRY

COMMUNICATION

View Article Online
View Journal | View Issue

Cite this: *Energy Adv.*, 2024, 3, 778

Received 21st January 2024,
Accepted 19th March 2024

DOI: 10.1039/d4ya00038b

rsc.li/energy-advances

A membrane electrode assembly-type cell designed for selective CO production from bicarbonate electrolyte and air containing CO_2 mixed gas†

Akina Yoshizawa,[a] Manabu Higashi,[a] Akihiko Anzai[a] and Miho Yamauchi *[abcd]

The electrochemical CO_2 reduction reaction (CO_2RR) combined with direct air capture (DAC) based CO_2 is a promising method for terrestrial carbon cycling. In this study, we have designed an all-Ag cathode and constructed a membrane electrode assembly (MEA) cell to utilize CO_2 capture solution, which can be produced by flowing air containing CO_2 mixed gas into an alkaline solution. A MEA consisting of a Ag nanoparticle catalyst sprayed on a Nafion membrane and a Ag electrode were used to construct a MEA cell (Ag MEA-cell). The Ag MEA-cell exhibited selective CO production without severe side reactions, such as the hydrogen evolution reaction, even when an aqueous electrolyte was used. The operation of the Ag MEA-cell using CO_2 capture solution, which was prepared by bubbling 60% air containing CO_2 mixed gas (40% CO_2 and 60% air, air–CO_2) into 1 M KOH, achieved CO production with 86% faradaic efficiency (FE_{CO}). Furthermore, the Ag MEA-cell significantly suppressed O_2 reduction and achieved FE_{CO} of 74% even when air–CO_2 was used as a CO_2 source.

Introduction

Carbon capture and utilization (CCU) of dilute atmospheric CO_2 and industrial exhaust gas is a key to efficient carbon cycling on earth,[1,2] and electrochemical CO_2 reduction reactions (CO_2RRs) using captured CO_2 are attracting much attention for the production of chemical feedstocks and fuels from CO_2.[3,4] The research field of the CO_2RR has evolved substantially over the past decade, particularly with the development of a gas diffusion electrode (GDE) in fluidized cathode cells and membrane electrode assemblies (MEAs) to improve the activity, product selectivity, and durability of catalysts.[5–7] Direct air capture (DAC) is one of the attractive methods to extract CO_2 from the air.[8,9] Currently, several DAC systems have been developed; adsorption-based DAC, which uses an alkaline solvent or a porous solid adsorbent to capture CO_2 as a carbonate/bicarbonate or other CO_2 derivatives, and permeation-based DAC, which consists of a stepwise separation using a membrane (m-DAC).[10–13] Unlike the other DAC systems, m-DAC does not require the input of large amounts of thermal energy to desorb CO_2 from the adsorbent, although multi-step separation is necessary to produce highly concentrated CO_2. Thus, m-DAC combined with the CO_2RR using impure CO_2 that can be produced by the smaller steps of the m-DAC process, would bypass energy-intensive purification,[14–16] and dramatically reduce CCU costs; purification of dilute CO_2 gas costs \$70–\$100 per ton (Fig. 1).[17–20] Meanwhile, when using impure CO_2 containing O_2, the CO_2RR is completely blocked in a conventional flow type cell (Fig. 2a and Fig. S1, ESI†) due to the overwhelmingly superior oxygen reduction reaction ($O_2 + 2H_2O + 4e^- \rightarrow 4OH^-$, ORR) (Fig. S2, ESI†),[14,21–23] and therefore most of

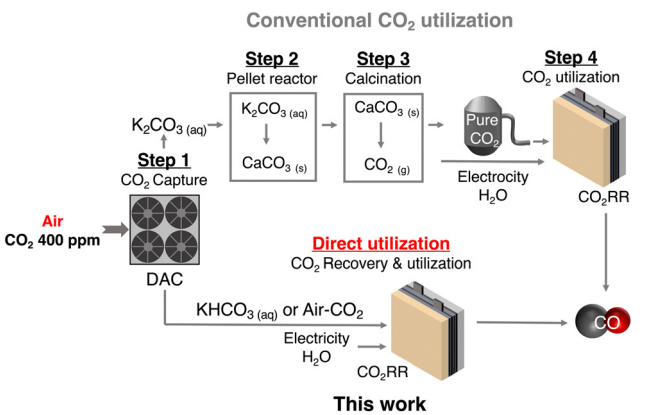

Fig. 1 Scheme of recovery and utilization of atmospheric CO_2.

[a] *Institute for Materials Chemistry and Engineering (IMCE), Kyushu University, Motooka 744, Nishi-ku, Fukuoka 819-0395, Japan. E-mail: yamauchi@ms.ifoc.kyushu-u.ac.jp*
[b] *Advanced Institute for Materials Research (WPI-AIMR), Tohoku University, 2-1-1 Katahira, Aoba-ku, Sendai 980-8577, Japan*
[c] *Research Center for Negative Emissions Technologies (K-NETs), Kyushu University, Motooka 744, Nishi-ku, Fukuoka 819-0395, Japan*
[d] *International Institute for Carbon-Neutral Energy Research (WPI-I²CNER), Kyushu University, Motooka 744, Nishi-ku, Fukuoka 819-0395, Japan*

† Electronic supplementary information (ESI) available. See DOI: https://doi.org/10.1039/d4ya00038b

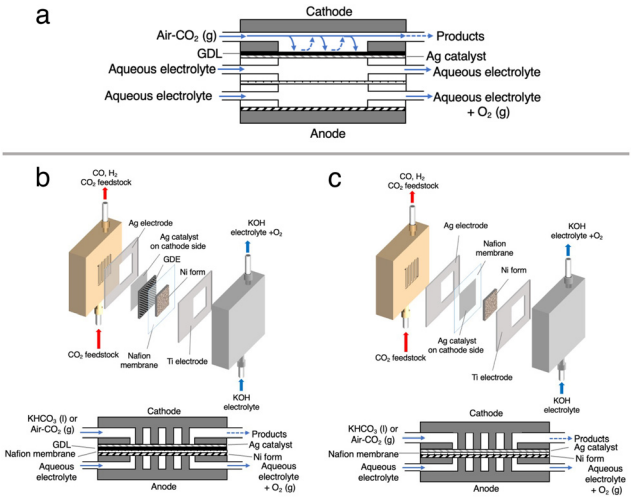

Fig. 2 Side view of (a) a conventional three-chamber cell, (b) the conventional MEA cell using a carbon based GDE and (c) the Ag MEA-cell. Parts with dots, gray oblique lines and black oblique lines are the membrane, cathode anode catalysts and carbon-based GDE, respectively. System configuration of (b) the conventional MEA-cell using GDE and (c) the Ag MEA-cell.

the CO_2RR research has been conducted using pure CO_2 gas (> 99%).[24–31] Interestingly, direct CO_2RR using air-containing mixed gas has been demonstrated using a newly designed flow cell consisting of a non-carbon gas diffusion layer (GDL),[14] but the products from the mixed gas still contain O_2 and N_2, and should be purified before use.

Recently, the CO_2RR using a bicarbonate solution, which is produced from DAC-captured CO_2 gas, has been in focus as an economically feasible CCU method. Here in this study, we explore efficient CO_2RR using O_2-containing CO_2 mixed gas that is captured by m-DAC. In this system, O_2 and N_2 are first removed by dissolving CO_2 in an alkaline solution to bicarbonate, which can be used as a CO_2 source and electrolyte. However, in a commonly used flow cell equipped with a carbon-based GDL, the HER is largely promoted when the bicarbonate solution is fed because carbon predominantly promotes the HER rather than the CO_2RR (Fig. 2b and Fig. S3, ESI†). To enhance the CO_2RR using a bicarbonate solution, we construct a membrane electrode assembly (MEA)-type cell equipped with two liquid flow channels at both the cathode and the anode. In particular, an all-Ag flow channel MEA cell (Ag MEA-cell) was newly designed for substrate diffusion, cathodic reactions and current collection to avoid severe hydrogen evolution reaction (HER) when aqueous solutions are flowing. We applied $KHCO_3$ solution prepared by bubbling a CO_2 mixed gas consisting of 40% CO_2 and 60% air (air–CO_2, where CO_2 is enriched by a factor of 1000) into an aqueous 3 M KOH solution. Furthermore, CO_2RR was demonstrated by directly introducing air–CO_2 to Ag MEA-cell.

Experimental section

Materials

The Ag nanoparticles (Ag NPs <100 nm in diameter) and Nafion™ perfluorinated resin solution (5 wt% in a mixture of low aliphatic alcohols and H_2O, containing 45% H_2O) were purchased from Sigma-Aldrich Co. LLC. Isopropanol (>99.7%), $KHCO_3$ (99%), KOH (>85%), and K_2CO_3 (99%) were obtained from FUJIFILM Wako Pure Chemical Corporation. All chemicals were used as received without further purification. Nafion™ 117 membrane was provided by Chemours. The Ag sheet and the titanium foil were purchased from the Nilaco Corporation. Nickel foam (1.6 mm thick, purity >99.99%) was obtained from MTI Corporation. Oxygen (>99.9%), CO_2 (>99.5%), and N_2 (>99.9%) were provided by Fukuoka Oxygen Co., Ltd.

Preparation of MEA and construction of a flow cell

Cathode electrodes were prepared using a reported air-brushing method.[27] Cathodic catalyst ink was prepared by mixing Ag NPs (40 mg), isopropanol (200 μL), deionized H_2O (50 μL), and Nafion™ perfluorinated resin solution (80 μL). The ink was airbrushed to a piece of Nafion™ 117 membrane, and allowed to air dry naturally. Unless otherwise noted, the Ag NP-sprayed cathodes were prepared with a catalyst loading of 2.5 mg cm^{-2}. Then, the MEA consisted of a nickel foam anode and a Ag NP-sprayed Nafion™ 117 membrane was prepared (Ag-MEA, Fig. 2c). A Ag MEA-cell was constructed by placing Ag-MEA between a Ag cathode and a Ti anode, with a polyetheretherketone (PEEK) flow plate on the cathode side and a Ti-based flow plate on the anode side. Each electrode was surrounded by silicone rubber for electrical insulation and to seal each compartment.

Characterizations

The morphology of the electrodes was evaluated by scanning electron microscopy (SEM) using a JSM-IT100 (JEOL) at 15 kV. The structures of the electrodes were identified by powder X-ray diffraction (XRD) using a D2 Phaser (Bruker).

The electrochemical measurement

Electrocatalytic measurements were performed with an electrochemical test system 1280Z (Solartron) in a two-electrode setup (Fig. 2c). 1.0 M KOH aqueous solution was used as the anolyte and fed to the anode compartment of the Ag MEA-cell at a flow rate of 1.0 mL min^{-1}. The cathode compartment was fed with $KHCO_3$ solution (BCS) at a flow rate of 1.0 mL min^{-1} or reactant gases at a flow rate of 15 ccm. The current density (J) on Ag MEA-cell was calculated based on the Ag cathode area covering Ag-MEA. Gas products were quantified by using a Micro GC FUSION (INFICON). The absence of liquid product was confirmed by high performance liquid chromatography (HPLC) using LC-20AD (Shimadzu) equipped with an RID-10A refractive index detector (Shimadzu). From gas chromatography (GC) and HPLC, no products other than CO and H_2 were detected by GC or HPLC. Resistance values for Ag MEA-cells were measured using the 1280Z electrochemical test system. The faradaic efficiencies (FE) were investigated in the cell voltage range of 1.8 to 2.4 V. The FEs for the production of CO (FE_{CO}) and H_2 (FE_{H_2}) were calculated according to the report and the representative results in several experimental tests are shown in this paper.[29] Because the size of the cell components was nearly

identical, the measured resistances without iR correction were directly used for discussion.

Results and discussion

CO_2RR using a bicarbonate solution

We first tested the CO_2RR on a typical MEA cell (Fig. 2b) with Ag NPs applied on a carbon-based gas diffusion electrode (GDE). Chronoamperometry was conducted by flowing 1.0 M BCS as a simulated CO_2-captured solution to the cathode side at a flow rate of 1.0 mL min^{-1} and 1.0 M KOH to the anode side at a flow rate of 1.0 mL min^{-1}. Fig. S3 (ESI†) represents that the FE_{H2} and FE_{CO} values on the MEA cell at 2.0 V of the cell voltage are 16 and 63%, respectively, indicating that the CO_2RR can proceed on a carbon-based GDE although the HER is still not negligible in the voltage range between 2.0 and 2.6 V.[26,32] It should be noted that the total FE did not reach 100% because of the difficulty in precisely controlling H_2 uptake at relatively low potentials in our experimental setup. At a voltage higher than 2.4 V, the HER was further promoted. Several authors have reported that a high overpotential is required to initiate the CO_2RR on the carbon-based GDE where the HER is predominant,[14,33] and therefore, we constructed a Ag MEA-cell without using a carbon-based GDE (Fig. 2c). Two flow plates with serpentine channels were used to supply 1.0 M KOH and 1.0 M BCS to the anode and the cathode, respectively. We used a PEEK channel to flow BCS on the cathode side because metal electrodes usually promote the HER in CO_2RR conducted in an aqueous electrolyte.[34,35] In addition, a Ag sheet with a square window was used as the electrode on the cathode side to minimize the contact between the electrode and electrolyte solution (Fig. 2c and 3a). SEM observation confirmed that the surface of the Nafion membrane was uniformly covered with Ag NPs without delamination and significant agglomeration (Fig. 3b–d).

We evaluated the CO_2RR performance of the Ag MEA-cell using BCS and found that CO and H_2 were the only detectable cathodic products based on the analysis of the outlet gas and electrolyte at the cathode compartment. The SEM images of the cathode side of the MEA before and after the reaction showed minimal change in surface morphology during the reaction (Fig. 3c and d). The X-ray diffraction (XRD) pattern of the Ag NPs on the starting MEA indicated characteristic peaks at 38.3, 44.5, 64.7 and 77.7°, corresponding to diffractions from the (111), (200), (220) and (311) planes of Ag, respectively and there was no change in the XRD patterns of the Ag NPs on the MEA before and after the reaction. These results confirmed that the Ag NPs on the cathode maintained their structure under our experimental conditions (Fig. S4 and Table S1, ESI†).

Fig. S5a (ESI†) shows the J, FE_{CO} and FE_{H2} in the CO_2RR using 1 M BCS in the voltage range between 1.8 and 2.4 V. As the cell voltage increased, the J gradually increased from 12.2 mA cm^{-2} at 1.8 V to 59.0 mA cm^{-2} at 2.4 V. Thus, the CO_2RR using BCS was achieved at voltages much lower than 3.0 V and previously reported voltages using a bipolar membrane (BPM).[36–38] At 2.0 V, FE_{H2} became minimal (FE_{H2} = 9.2%),

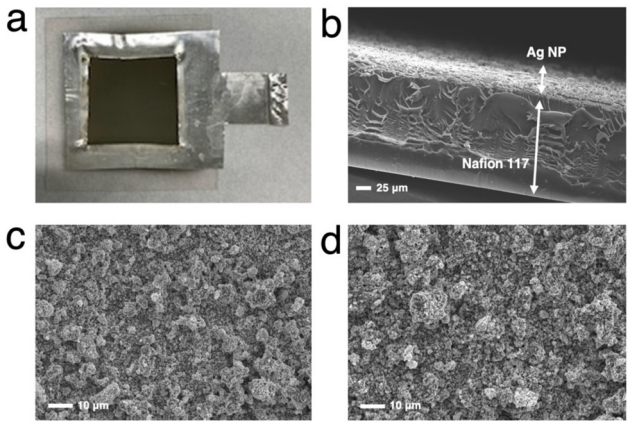

Fig. 3 (a) A photograph of the MEA for the Ag MEA-cell and (b) the cross-section SEM image of the MEA with 2.5 mg cm^{-2} of Ag NPs. SEM images of the Ag NPs coated on the MEA (c) before and (d) after the CO_2RR in BCS.

whereas FE_{CO} increased to FE_{CO} = 93% with J = 27 mA cm^{-2}, suggesting that a more selective CO_2RR occurs compared to those on MEA cells with a carbon-based GDE (FE_{H_2} = 16% and FE_{CO} = 63% with J = 30.9 mA cm^{-2} at 2.0 V, Fig. S3, ESI†). Considering that 3 M BCS is the almost saturated one, we performed the CO_2RR using 2 M and 3 M BCSs to increase the efficiency (Fig. 4a and Fig. S5b, ESI†). When 2 M BCS was flowed, we achieved the best performance with FE_{CO} > 99% and J = 51.5 mA cm^{-2} at 2.1 V (Fig. 4a), indicating that almost pure CO was obtained as a CO_2RR product. The high selectivity and good J in the CO_2RR using 2 M BCS are possibly related to the appropriate balance between the BCS concentration and the solution resistances; 1, 2 and 3 M BCS showed resistances of 1.31, 2.17 and 3.08 Ω, respectively. A comparison of the performance found here with the reported results is summarized in Table S3 (ESI†).

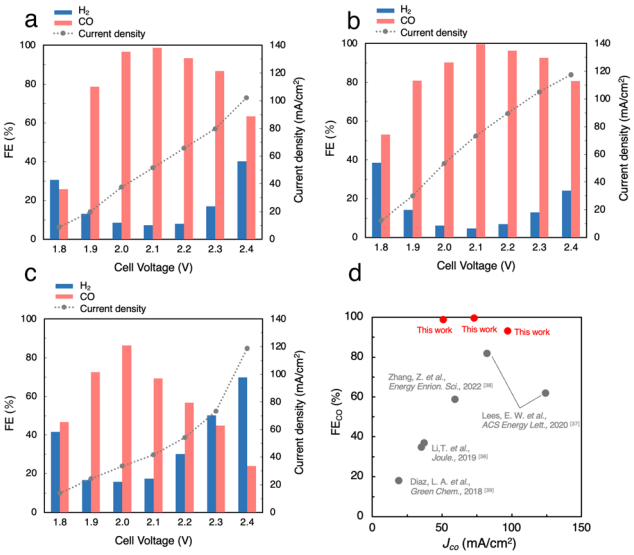

Fig. 4 Faradaic efficiency (FE) and current density (J) for the CO_2RR using (a) 2.0 M BCS and (b) CO_2-sol and (c) air–CO_2-sol. (d) Comparison of state-of-the-art performances for the CO_2RR using BCS coupled with CO_2 capture.

CO_2RR using a CO_2 capture solution

Next, we performed the CO_2RR by flowing a CO_2 capture solution, which was prepared by bubbling pure CO_2 gas into 1.0 M KOH (CO_2-sol, pH 7.55, Table S2, ESI†) as the electrolyte, and achieved $FE_{CO} > 99\%$ and $J = 73.3$ mA cm^{-2} at 2.1 V (Fig. 4b). Interestingly, FE_{CO} remained at 93% even with a relatively high $J = 105$ mA cm^{-2} at 2.3 V, which implies that the J values in the CO_2RR using CO_2-sol are higher than those in BCSs. The reported MEA cells using BCS mostly used a BPM, which requires a large overpotential of more than 3.0 V for the dissociation of H_2O into H^+ and OH^- at the membrane ($H_2O(l) \rightleftharpoons H^+(aq) + OH^-(aq)$).[36–38] In contrast, our Ag MEA-cell made of a Nafion membrane can eliminate the need for H_2O dissociation. Furthermore, the Ag MEA-cell showed higher FE_{CO} and higher J compared to the previously reported performances, which exhibits great potential of CO_2RRs for the direct utilization of BCS as a CO_2 resource.[36–39]

We then demonstrated the CO_2RR using a CO_2 capture solution prepared by bubbling air–CO_2 into 3 M KOH (air–CO_2-sol). The pH of air–CO_2-sol was 7.90 (Table S2, ESI†), indicating that bicarbonate is the primary carbon species in air–CO_2-sol.[40] A high FE_{CO} of 86% with $J = 33.4$ mA cm^{-2} in the CO_2RR using air–CO_2-sol was realized at 2.0 V (Fig. 4c), indicating that the Ag MEA-cell exhibits significantly high selectivity for CO production even using air–CO_2-sol and a high possibility for direct utilization of various impure CO_2 sources.

CO_2RR using 60% air containing CO_2

We tried to directly apply air–CO_2 as a reactant gas to Ag MEA-cell. As mentioned above, the inclusion of O_2 in the reactant gas is known to completely inhibit the progress of the CO_2RR in a conventional electrochemical flow cell due to highly preferential ORR.[14,22] In fact, we performed the CO_2RR by feeding air–CO_2 into a conventional flow cell using a carbon-based GDE on which Ag NPs were applied (Fig. 2a and Fig. S1, ESI†),[23,26,32] but did not observe any products, neither CO nor H_2 (Fig. S2, ESI†). This result implies that CO_2 does not interact with the Ag catalyst on the carbon GDE in the presence of air and that the current flowing into the GDE is predominantly used for the ORR before the onset of the CO_2RR, which is explained by the fast kinetics of the ORR.[41–44] It should be recalled that the newly designed Ag MEA-cell has a unique structure in which the reactant gas can directly contact the Ag NP catalyst, implying the possibility of the CO_2RR on Ag MEA-cell even with air–CO_2. Before investigating the CO_2RR with air–CO_2, the CO_2RR performance on the Ag MEA-cell was examined by flowing pure CO_2 to the cathode side. Fig. S6 (ESI†) represents that J increases with increasing cell voltage, reaching 100 mA cm^{-2} at 2.3 V and the CO_2RR using pure CO_2 gas shows more than 2 times better J between 2.0 and 2.4 V compared to the CO_2RR using 1 M BCS. The voltage was considerably small compared to the reported voltage of 3.5 V on a BPM-equipped MEA cell showing the large overpotential on a BPM to dissociate H_2O into H^+ and OH^-.[45–47] Furthermore, we achieved $FE_{CO} = 97\%$ at 2.3 V and $J = 100$ mA cm^{-2} using the optimized Nafion loading on Ag-MEA (Fig. S7 and S8a, ESI†).

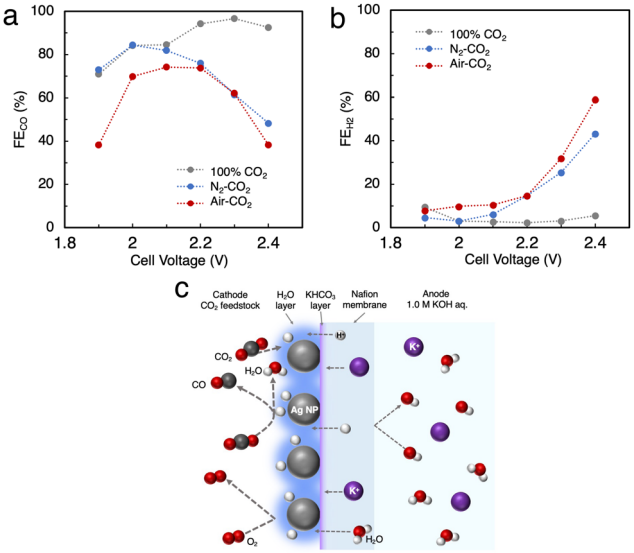

Fig. 5 (a) FE for CO production (FE_{CO}) and (b) for the HER (FE_{H_2}) in the CO_2RR using N_2-CO_2 and air–CO_2. (c) Predicted mechanism of the CO_2RR on the Ag MEA-cell.

To investigate the effect of CO_2 concentration, we used a mixed gas consisting of 40% CO_2 and 60% N_2 (N_2-CO_2) for the CO_2RR in the voltage range of 2.0 to 2.4 V with 10% Nafion loading on Ag-MEA under the optimized conditions (Fig. S8b, ESI†). We found that the selectivity for the CO_2RR is significantly reduced when using N_2-CO_2, especially at higher cell voltages above 2.3 V (Fig. 5a and b). For example, the FE_{CO} was reduced to 48% at 2.4 V compared to $FE_{CO} = 93\%$ at 2.4 V for pure CO_2, whereas FE_{H_2} was significantly increased to 43%, suggesting that the HER is promoted at low CO_2 concentration.

Subsequently, air–CO_2 was used as a CO_2 source to examine the effect of O_2 inclusion on the CO_2RR. The CO_2RR in the Ag MEA-cell reached $FE_{CO} = 74\%$ and $J = 56.7$ mA cm^{-2} at 2.2 V (Fig. S8c, ESI†), which is analogous to $FE_{CO} = 76\%$ and $J = 39.9$ mA cm^{-2} at 2.2 V for N_2–CO_2 (Fig. S8b, ESI†), indicating that the decrease in FE_{CO} is caused by the low CO_2 concentration, not by the enhancement of the ORR. When the CO_2RR was performed above 1.9 V, the total FE values or the sum of FE_{CO} and FE_{H_2} became less than 100%, which suggests that a part of the flowed current is used for the ORR, and the HER was increased above 2.3 V. Thus, the favorable FE_{CO} in the CO_2RR with using air–CO_2 between 2.0 and 2.2 V is possibly explained by the previously reported phenomenon;[42] a thin layer of H_2O is formed on the Ag catalyst surface by the ORR, which prevents O_2 from contacting the Ag catalyst surface as shown in Fig. 5c. In addition, the H_2O produced by the ORR increases the moisture content of the Nafion membrane, which reduces its insulating properties and results in a relatively high J value.

Conclusion

The newly constructed Ag MEA-cell significantly suppresses the HER, which makes it applicable to the CO_2RR using BCS.

Table 1 The summary of the CO_2RR results using various CO_2 sources

Entry	CO_2 source	Cell voltage (V)	FE_{CO} (%)	J (mA cm^{-2})
1	2 M BCS	2.1	>99	51.5
2	CO_2-sol	2.1	>99	73.3
3	Air–CO_2-sol	2.0	86	33.4
4	CO_2	2.3	97	100
5	Air–CO_2	2.2	74	56.7

After the detailed optimization of the reaction conditions, we have achieved the maximum $FE_{CO} > 99\%$ and partial current density for CO production (J_{CO}) of 73.3 mA cm^{-2} in the CO_2RR using 1.0 M CO_2-sol. Even when we used air–CO_2-sol, high CO selectivity FE_{CO} = 86% with 33.4 mA cm^{-2} was achieved at 2.0 V (Table 1). Furthermore, excellent CO selectivity with FE_{CO} = 74% and relatively high J = 52.7 mA cm^{-2} were realized by direct application of air–CO_2 to Ag MEA-cell, suggesting a selective CO_2RR with suppressed ORR even using air–CO_2 due to the unique structure of the Ag MEA-cell where the contact points between air–CO_2 and the electrode were minimized. These results showed that the Ag MEA-cell structure has high potential for the direct conversion of CO_2 feedstocks captured by DAC, which would broaden the applicability of the combination of DAC and CO_2RR technologies.

Author contributions

A. Y. and M. H. designed the experiments and M. Y. supervised the project. M. H. performed the electrolyzer experiments. A. A and A. Y. measured XRD, and A. A., A. Y. and M. H. measured SEM of the MEAs. A. Y. and M. H. defined the reactions in the flow cell. A. Y. performed the data analysis. A. Y. wrote the first manuscript draft and all authors contributed to manuscript writing.

This work was supported by NEDO the Moonshot Research and Development Program (JPNP18016) and JSPS KAKENHI (JP22K19088, JP23H00313).

Conflicts of interest

The authors declare no competing financial interest.

Notes and references

1 J. Artz, T. E. Müller, K. Thenert, J. Kleinekorte, R. Meys, A. Sternberg, A. Bardow and W. Leitner, *Chem. Rev.*, 2018, **118**, 434–504.
2 H.-J. Ho, A. Iizuka and E. Shibata, *Ind. Eng. Chem. Res.*, 2019, **58**(21), 8941–8954.
3 J. Qiao, Y. Liu, F. Hong and J. Zhang, *Chem. Soc. Rev.*, 2014, **43**, 631–675.
4 O. G. Sánchez, Y. Birdja, M. Bulut, J. Vaes, T. Breugelmans and D. Pant, *Curr. Opin. Green Sustainable Chem.*, 2019, **16**, 47–56.
5 G. Díaz-Sainz, M. Alvarez-Guerra, B. Ávila-Bolívar, J. Solla-Gullónb, V. Montiel and A. Irabiena, *J. Chem. Eng.*, 2021, **405**, 126965.
6 W. Lee, Y. E. Kim, M. H. Youn, S. K. Jeong and K. T. Park, *Angew. Chem., Int. Ed.*, 2018, **57**, 6883–6887.
7 Y. C. Li, G. Lee, T. Yuan, Y. Wang, D.-H. Nam, Z. Wang, F. P. García de Arquer, Y. Lum, C.-T. Dinh, O. Voznyy and E. H. Sargent, *ACS Energy Lett.*, 2019, **4**(6), 1427–1431.
8 E. S. Sanz-Pérez, C. R. Murdock, S. A. Didas and C. W. Jones, *Chem. Rev.*, 2016, **116**(19), 11840–11876.
9 A. Sodiq, Y. Abdullatif, B. Aissa, A. Ostovar, M. Nassar, M. El-Naas and A. Amhamed, *Environ. Technol. Innov.*, 2023, **29**, 102991.
10 O. Selyanchyn, R. Selyanchyn and S. Fujikawa, *ACS Appl. Mater. Interfaces*, 2020, **12**(29), 33196–33209.
11 S. Fujikawa, R. Selyanchyn and T. Kunitake, *Polym. J.*, 2021, **53**, 111–119.
12 S. Fujikawa and R. Selyanchyn, *MRS Bull.*, 2022, **47**, 416–423.
13 R. Castro-Muñoz, M. Z. Ahmad, M. Malankowska and J. Coronas, *J. Chem. Eng.*, 2022, **446**(2), 137047.
14 A. Anzai, M. Higashi and M. Yamauchi, *Chem. Commun.*, 2023, **59**, 11188–11191.
15 D. M. D'Alessandro, B. Smit and J. R. Long, *Angew. Chem., Int. Ed.*, 2010, **49**, 6058–6082.
16 M. E. Boot-Handford, J. C. Abanades, E. J. Anthony, M. J. Blunt, S. Brandani, N. Mac Dowell, J. R. Fernández, M.-C. Ferrari, R. Gross, J. P. Hallett, R. S. Haszeldine, P. Heptonstall, A. Lyngfelt, Z. Makuch, E. Mangano, R. T. J. Porter, M. Pourkashanian, G. T. Rochelle, N. Shah, J. G. Yao and P. S. Fennell, *Energy Environ. Sci.*, 2014, **7**, 130–189.
17 M. T. Ho, G. W. Allinson and D. E. Wiley, *Energy Procedia*, 2009, **1**, 763–770.
18 R. F. Service, *Science*, 2016, **354**, 1362–1363.
19 B. Kim, S. Ma, H.-R. M. Jhong and P. J. A. Kenis, *Electrochim. Acta*, 2015, **166**, 271–276.
20 M. Erans, E. S. Sanz-Pérez, D. P. Hanak, Z. Clulow, D. M. Reiner and G. A. Mutch, *Energy Environ. Sci.*, 2022, **15**, 1360–1405.
21 D. Kim, W. Choi, H. W. Lee, S. Y. Lee, Y. Choi, D. K. Lee, W. Kim, J. Na, U. Lee, Y. J. Hwang and D. H. Won, *ACS Energy Lett.*, 2021, **6**, 3488–3495.
22 S. Polani, N. Kanovsky and D. Zitoun, *ACS Appl. Nano Mater.*, 2018, **1**, 3075–3079.
23 F. Li, C. Zhou, E. Feygin, P.-N. Roy, L. D. Chen and A. Klinkova, *Phys. Chem. Chem. Phys.*, 2022, **24**, 19432–19442.
24 M. R. Thorson, K. I. Siil and P. J. A. Kenis, *J. Electrochem. Soc.*, 2013, **160**, F69.
25 B. Kim, S. Ma, H.-R. M. Jhong and P. J. A. Kenis, *Electrochim. Acta*, 2015, **166**, 271–276.
26 S. Ma, R. Luo, J. I. Gold, A. Z. Yu, B. Kim and P. J. A. Kenis, *J. Mater. Chem. A*, 2016, **4**(22), 8573–8578.
27 S. Ma, M. Sadakiyo, R. Luo, M. Heima, M. Yamauchi and P. J. A. Kenis, *J. Power Sources*, 2016, **301**, 219–228.
28 S. Ma, M. Sadakiyo, M. Heima, R. Luo, R. T. Haasch, J. I. Gold, M. Yamauchi and P. J. A. Kenis, *J. Am. Chem. Soc.*, 2017, **139**(1), 47–50.
29 A. Anzai, M.-H. Liu, K. Ura, T. G. Noguchi, A. Yoshizawa, K. Kato, T. Sugiyama and M. Yamauchi, *Catalysts*, 2022, **12**, 478.

30 M. Sun, A. Staykov and M. Yamauchi, *ACS Catal.*, 2022, **12**(24), 14856–14863.
31 M. Sun, J. Cheng and M. Yamauchi, *Nat. Commun.*, 2024, **15**, 491.
32 Q. Lu, J. Rosen, Y. Zhou, G. S. Hutchings, Y. C. Kimmel, J. G. Chen and F. Jiao, *Nat. Commun.*, 2014, **5**, 3242.
33 K. Yang, R. Kas, W. A. Smith and T. Burdyny, *ACS Energy Lett.*, 2021, **6**, 33–40.
34 Y. Hori, H. Wakebe, T. Tsukamoto and O. Koga, *Electrochim. Acta*, 1994, **39**, 1833–1839.
35 Y. J. Sa, C. W. Lee, S. Y. Lee, J. Na, U. Lee and Y. J. Hwang, *Chem. Soc. Rev.*, 2020, **49**, 6632–6665.
36 T. Li, E. W. Lees, M. Goldman, D. A. Salvatore, D. M. Weekes and C. P. Berlinguette, *Joule*, 2019, **3**, 1487–1497.
37 E. W. Lees, M. Goldman, A. G. Fink, D. J. Dvorak, D. A. Salvatore, Z. Zhang, N. W. X. Loo and C. P. Berlinguette, *ACS Energy Lett.*, 2020, **5**, 2165–2173.
38 Z. Zhang, E. W. Lees, F. Habibzadeh, D. A. Salvatore, S. Ren, G. L. Simpson, D. G. Wheeler, A. Liu and C. P. Berlinguette, *Energy Environ. Sci.*, 2022, **15**, 705–713.
39 L. A. Diaz, N. Gao, B. Adhikari, T. E. Lister, E. J. Dufek and A. D. Wilson, *Green Chem.*, 2018, **20**, 620–626.
40 J. Zosel, W. Oelßner, M. Decker, G. Gerlach and U. Guth, *Meas. Sci. Technol.*, 2011, **22**, 072001.
41 M. Chatenet, L. Genies-Bultel, M. Aurousseau, R. Durand and A. Andolfatto, *J. Appl. Electrochem.*, 2002, **32**, 1131–1140.
42 L. Tammeveski, H. Erikson, A. Sarapuu, J. Kozlova, P. Ritslaid, V. Sammelselg and K. Tammeveski, *Electrochem. Commun.*, 2012, **20**, 15–18.
43 Z. Chen, C. Li, Y. Ni, F. Kong, Y. Zhang, A. Kong and Y. Shan, *Electrochim. Acta*, 2017, **239**, 45–55.
44 H. Erikson, A. Sarapuu and K. Tammeveski, *ChemElectroChem*, 2019, **6**, 73–86.
45 D. A. Salvatore, D. M. Weekes, J. He, K. E. Dettelbach, Y. C. Li, T. E. Mallouk and C. P. Berlinguette, *ACS Energy Lett.*, 2018, **3**, 149–154.
46 C. P. O'Brien, R. K. Miao, S. Liu, Y. Xu, G. Lee, A. Robb, J. E. Huang, K. Xie, K. Bertens, C. M. Gabardo, J. P. Edwards, C.-T. Dinh, E. H. Sargent and D. Sinton, *ACS Energy Lett.*, 2021, **6**, 2952–2959.
47 K. Yang, M. Li, S. Subramanian, M. A. Blommaert, W. A. Smith and T. Burdyny, *ACS Energy Lett.*, 2021, **6**, 4291–4298.